2022-08-15

Fe0-Supported Anaerobic Digestion for Organics and Nutrients Removal from Domestic Sewage

Bakari, Omari

Article

Fe^0-Supported Anaerobic Digestion for Organics and Nutrients Removal from Domestic Sewage

Omari Bakari [1], **Karoli N. Njau** [1] **and Chicgoua Noubactep** [2,3,4,*]

1   School of Materials, Energy, Water and Environmental Sciences, Nelson Mandela African Institution of Science and Technology (NM-AIST), Arusha 23311, Tanzania; bakario@nm-aist.ac.tz (O.B.); karoli.njau@nm-aist.ac.tz (K.N.N.)
2   Centre for Modern Indian Studies (CeMIS), University of Göttingen, Waldweg 26, D-37073 Göttingen, Germany
3   School of Earth Science and Engineering, Hohai University, Fo Cheng Xi Road 8, Nanjing 211100, China
4   Faculty of Science and Technology, Campus of Banekane, Université des Montagnes, Bangangté P.O. Box 208, Cameroon
*   Correspondence: cnoubac@gwdg.de

Abstract: Results from different research suggest that metallic iron (Fe^0) materials enhance anaerobic digestion (AD) systems to remove organics (chemical oxygen demand (COD)), phosphorus and nitrogen from polluted water. However, the available results are difficult to compare because they are derived from different experimental conditions. This research characterises the effects of Fe^0 type and dosage in AD systems to simultaneously remove COD and nutrients (orthophosphate (PO$_4^{3-}$), ammonium (NH$_4^+$), and nitrate (NO$_3^-$)). Lab-scale reactors containing domestic sewage (DS) were fed with various Fe^0 dosages (0 to 30 g/L). Batch AD experiments were operated at $37 \pm 0.5\ ^\circ$C for 76 days; the initial pH value was 7.5. Scrap iron (SI) and steel wool (SW) were used as Fe^0 sources. Results show that: (i) SW performed better than SI on COD and PO$_4^{3-}$ removal (ii) optimum dosage for the organics and nutrients removal was 10 g/L SI (iii) (NO$_3^-$ + NH$_4^+$) was the least removed pollutant (iv) maximum observed COD, PO$_4^{3-}$ and NO$_3^-$ + NH$_4^+$ removal efficiencies were 88.0%, 98.0% and 40.0% for 10 g/L SI, 88.2%, 99.9%, 25.1% for 10 g/L SW, and 68.9%, 7.3% and 0.7% for the reference system. Fe^0-supported AD significantly removed the organics and nutrients from DS.

Keywords: anaerobic digestion; domestic sewage; metallic iron; organics and nutrients

1. Introduction

Anaerobic wastewater treatment systems are commonly used in developing countries due to: simplicity, low construction, operation and maintenance costs, and facilitating recovery of resources from wastes. However, conventional systems achieve poor to moderate effluent quality and have a more extended start-up period [1,2]. The effluents from anaerobic reactors require polishing to further remove residual COD for compliance [3,4]. On the other hand, nitrogen (N) and phosphorus (P) are common contaminants found in significant concentrations in domestic sewage and may result in the eutrophication of surface water sources at a certain P to N ratio [5–7]. Different studies evaluated and suggested innovative approaches for improving the efficiency of anaerobic digestion. The approaches include pre-treatment co-digestion, digester design [8–10], and additives' application of additives [11]. The additives include (i) ashes from waste incineration, (ii) the supplements of macro- (e.g., P, N, and sulphur (S)) and micro- (cobalt (Co), iron (Fe), molybdenum (Mo), nickel (Ni), selenium (Se), and tungsten (W)) nutrients (iii) compounds (e.g., bentonite, glauconite, phosphorite, and zeolites) capable of mitigating ammonia inhibition (iv) bioaugmentation and (v) compounds (e.g., Fe^0 and Fe^{III}) with high biomass immobilisation capacity [11].

Metallic iron (Fe^0), as an efficient additive in Fe^0-amended anaerobic digestion systems, have been reported to enhance the performance of anaerobic systems in removing organics and nutrients [12–14]. Fe^0-amended anaerobic digestion systems have been linked with the following performances: (i) increasing the efficiency of hydrolysis and acidogenesis and the production of methane in the digestion of waste activated sludge [15]; (ii) increased the overall performance in the digestion of food wastes [16]; (iii) preventing excessive acidification in the digestion of food wastes [16,17]; (iv) enriching methane of biogas in the digestion of palm oil mill effluent [18] (v) enhancing the conversion of propionate to acetate [19]; and (vi) enhancing the COD removal and methane production in the treatment of swine wastewater [12]. On the other hand, Fe^0 materials have been reported to play a role as a cofactor of different enzymatic activities, facilitating fermentation and providing a more favourable environment for anaerobic digestion due to their ability to decrease the oxidative-reductive potential of anaerobic digestion media [20]. Moreover, Fe^0 materials accelerate the hydrolysis and fermentation stages [21]; enhance the production of more soluble organics during the hydrolysis process, regulate acidification in anaerobic digestion [22]; enhance the reduction in the accumulation of propionate, the unfavourable substrate in anaerobic digestion [19].

Furthermore, the potential of the Fe^0 materials to remove nutrients from wastewater has been reported in different researches: (i) Fe^0-supported autotrophic denitrification is a promising technology in the treatment of low carbon wastewater [13,23] (ii) the reactor fed with the steel wool and *P. denitrificans* denitrified 64% of the added NO_3^- to N_2O, and reduced only 28% of it to ammonium [23] (iii) According to Tchobanoglous [6], phosphate removal can be realised through adsorption by hydrous ferric, phosphate incorporation into the structure of hydrous oxide, and formation of ferric phosphates that are removed as precipitates. For improving the performance of anaerobic wastewater treatment systems, Fe^0 material has been acknowledged as one of the prominent additives due to its abundance, affordability, non-toxicity, and worldwide availability (e.g., steel wool) [14,24–27].

In addition to the intrinsic characteristics of Fe^0 materials [28,29], the experimental operational parameters such as pH, dissolved oxygen (DO), iron dosage, iron pretreatment, mixing conditions, volume of the reactor used, volume of the added solution, contact time and temperature also influence the performance of the Fe^0 materials in pollutants removal [29–32]. One of the most important characteristics of wastewater that greatly affects the rate of pollutants removal by Fe^0 materials is the pH [29,30,32]. Different optimum pH ranges have been reported for different contaminants removal by Fe^0-supported biological wastewater treatment systems [29,30]. For instance, it was reported that: the highest removal of perchlorate was achieved at the pH of 7.0 and little if any reduction was observed at the pH of 6.0 or 9.0 [33,34]; the optimum pH of 7.6 to 8.4 was identified for the ammonium nitrogen (NH_4^+-N) and total nitrogen (TN) removal in the biological denitrification process based on Fe^0–carbon micro-electrolysis denitrification [35]; in the bioremediation of copper-containing wastewater by sulphur reducing bacterial coupled with Fe^0, the 99% total sulfate removal was achieved at pH 4.0 t0 7.0 [36].

Many types of research on the Fe^0-supported anaerobic digestion focused on the mechanisms and improving stages of the anaerobic digestion pathway (hydrolysis, acidogenesis, acetogenesis, and methanogenesis) for different types of organic wastes [21,30,37]. Moreover, with different wastewaters, few researchers separately studied nitrate or phosphorus removal by Fe^0. Similarly, in the review article by Xu [30], it was revealed that most of the studies on the integration of Fe^0 in the anaerobic digestion of wastewater focused on one type of pollutant with a relatively high concentration. Additionally, the available results were derived from experiments performed under very different conditions and thus difficult to compare. No study has compared the significance of Fe^0-supported anaerobic digestion system in the simultaneous removal of organics (COD) and nutrients (PO_4^{3-} and $NO_3^- + NH_4^+$) from domestic sewage.

On the other hand, each Fe^0 material has its intrinsic reactivity [28,38,39]. For this reason, different performances are expected in Fe^0–supported effluent treatment systems

using different Fe^0 specimens for the treatment of the same effluent. However, the significances of the differences are also difficult to compare based on the available results because the available results were also derived from experiments performed under very different conditions. Therefore, different performances of the tested Fe^0-supported anaerobic digestion systems in pollutants (PO_4^{3-} and $NO_3^- + NH_4^+$) removal from domestic sewage were expected in this study due to the following; (i) different types of the Fe^0 materials (SI and SW) tested and (ii) varied dosages of SI materials

This study compares Fe^0 types and dosages on the simultaneous removal of organics (COD) and nutrients (PO_4^{3-} and $NO_3^- + NH_4^+$) from domestic sewage. The experiment involved the anaerobic batch reactors operated at 37 ± 0.5 °C for 76 days. The samples collected from the tested Fe^0-supported anaerobic batch reactors and the reference system (reactor without Fe^0) were analysed for PO_4^{3-} and $NO_3^- + NH_4^+$ to compare the systems' significances in the pollutants removal. The basis for comparison in the significance of the difference in performances between the systems were; (i) the difference in pollutants removal performance between the reactors dosed with Fe^0 materials (SI or SW) and the reference system, and (ii) between the reactor dosed with SI and that with SW materials. Selection of Fe^0 materials dosages (1, 4, 10, 15, and 30 g Fe^0/L) was based on experience. Fe^0 material dosages ranging from 0 to 50 g/L have been successfully applied in various research with less than 30 g Fe^0/L optimum dosages [12,18,40–43]. The research studies how significant the Fe^0-supported anaerobic system is in removing organics and nutrients from particular organic wastes (domestic sewage) as the contribution to the move toward using anaerobic digester as a unit for organics and nutrients removal.

2. Materials and Methods

2.1. Material

2.1.1. Sludge and Wastewater

Sludge used as the inoculum was collected from the operating septic tank treating domestic wastewater from the students' hostel at the Nelson Mandela African Institution of Science and Technology (NM-AIST). The sludge had a pH of 6.8, COD of 3.425 gCOD/L, tototal solids (TS) of 12.85 gTS/L, total volatile solids (TVS) of 7.71 gVS/L, volatile suspended solids (VSS) of 5.25 gVSS/L, total phosphorus (TP) of 165 mg P/L, and total kjeldahl nitrogen (TKN) of 885 mg/L.

The wastewater used in this study was collected below the scum layer at the inlet zone of the septic tank to avoid as much as possible the floating objects, oil, and grease. The wastewater had the following characteristics: pH of 7.5, COD of 408 mg COD/L, PO_4^{3-} of 17.8 mg PO_4^{3-}/L, NO_3^- of 19.8 mg NO_3^-/L, and NH_4^+ of 53.1 mg NH_4^+/L.
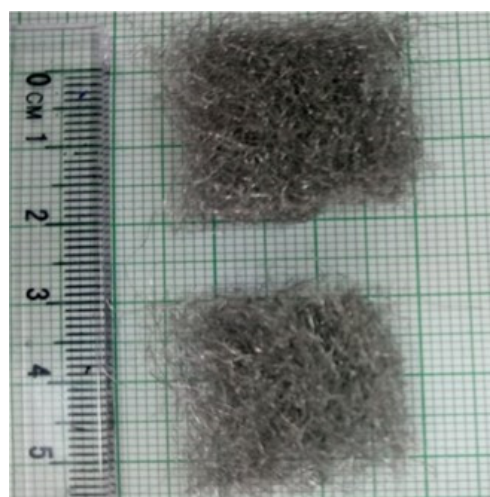
2.1.2. Fe^0 Materials

The Fe^0 materials used in this study were scrap iron and commercial steel wool with product code FGSK003. The materials were used in this experiment because they are readily available, cheap, and their reactivities based on the past experiments [28,44]. The scrap iron materials were generated from the lathing machine at Mbeya University of Science and Technology (MUST, Mbeya, Tanzania), while Steel wool (Africa) Limited (Nairobi, Kenya) manufactures the commercial steel wool product. Both materials were not protected from air oxidation. The steel wool materials used had an iron content of 99.25%, while the scrap iron materials had 98.68% (Table 1). The elemental composition of the Fe^0 materials was determined using Bruker S1 TITAN 800 XRF spectrometer (Bruker, Billerica, MA, USA). The steel wool material was cut into equal pieces of about 25 mm, while scrap iron ranged between 4 mm and 20 mm (Figure 1).

Table 1. Elemental composition of tested Fe^0 materials. LOD stands for the lowest concentration at which an element can be detected.

Name	Elemental Composition (%)							
	Fe	Cu	Ni	Cr	Mn	Sn	Nb	Mo
Steel wool (SW)	99.25	0.09	0.09	0.04	0.5	<LOD	<LOD	<LOD
Steel scraps (SI)	98.68	0.33	0.15	0.27	0.4	0.07	0.01	0.02
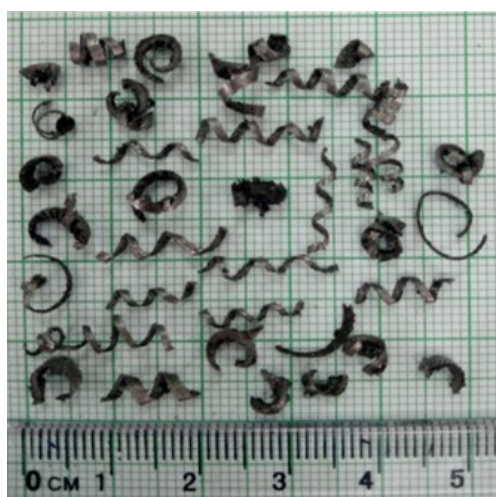
(a)　　　　　　　　　　　　　　　　　　　　　　　　　　　(b)

Figure 1. Size specification of Fe^0 materials tested—(**a**) Scrap iron (**b**) Steel wool.

2.2. Experimental Procedure

2.2.1. Fe^0 Reactivity

A dissolution experiment was performed using 0.1 g of each material (SW or SI) in 50 mL of 2 mM 1, 10 Phenanthroline for 120 h at an undisturbed condition. The materials were weighed and submersed into plastic bottles containing 50 mL of 1,10 Phenanthroline. There were no pre-treatments carried out to the materials before testing. The experiments were performed in triplicates and protected from sunlight [28]. The results of total iron concentrations presented are the average values.

2.2.2. Contaminants Removal

The study involved testing of nine different reactors described in Table 2. The reactors were fabricated using a PVC pipe with a nominal diameter of 110 mm. Each reactor had a total capacity of 3500 mL. Except for the two reactors (System VIII and System IX) that were fed with 3000 mL distilled water and Fe^0 materials, each of the other reactors (Systems I to VII) were fed with 3000 mL of domestic sewage, 300 mL of inoculum, and Fe^0 materials. All reactors were operated parallel in a water bath at quiescent conditions, batch mode, and a mesophilic temperature of 37 ± 0.5 °C. The systems II to VI are anaerobic reactors dosed with various amounts (Table 2) of SI materials to compare the effects of varying SI materials dosages in pollutants removal. The comparison between SI and SW materials' effect on pollutants removal was studied using systems IV and VII. Both systems (IV and VII) were fed with the same domestic sewage and dose but different types of Fe^0 materials (Table 2). The systems IV, VII, VIII and IX, were used to study the behaviour of Fe^0 materials (SI or SW) in domestic sewage. The distilled water medium was used for comparison purposes. Each of the systems (IV, VII, VIII and IX) was dosed with 10 g/L of Fe^0 materials but the different medium (DS or DW) or type of Fe^0 materials (SI or SW) (Table 2). The system I

was used as control (no Fe^0 materials added) for the systems (II to VII) treating domestic sewage (Table 2).

Table 2. Identities of reactors used in tested reactors. Each system contains 3000 mL of the medium (DS or DW). DS stands for domestic sewage, DW for distilled water, SI for scrap iron and SW for steel wool. The accuracy in measurements of Fe^0 materials' dosages was 0.1 mg Fe^0/L.

System	Medium	Fe^0 Material	Fe^0 Dosage (g/L)	Fe^0 to Inoculum Ratio (g Fe^0/gTS)
I	DS	none	0	0.00
II	DS	SI	1	0.08
III	DS	SI	4	0.31
IV	DS	SI	10	0.78
V	DS	SI	15	1.17
VI	DS	SI	30	2.33
VII	DS	SW	10	0.78
VIII	DW	SI	10	-
IX	DW	SW	10	-

Samples from the reactors (Systems I to IX) were taken through sampling ports controlled by a ball valve every second to the third day of operation. In order to assess pollutants removal performance, the samples were analysed for chemical oxygen demand (COD), nitrate (NO_3^-), orthophosphate (PO_4^{3-}), and ammonium (NH_4^+). Total Iron (Total-Fe) and pH were also for monitoring purposes. For systems VIII and IX, only the pH and Total-Fe were analysed to compare the medium's impact on the materials' dissolution and pH changes. The analysis of COD, NH_4^+, NO_3^-, PO_4^{3-} and Total-Fe followed the APHA recommended standard methods for examining wastewater.

2.3. Analytical Methods

The iron concentrations were determined using a DR2800 spectrophotometer manufactured by HACH Company in Berlin, Germany, at a wavelength of 510 nm using a 5 cm cuvette. The testing procedures were adopted from Lufingo [28] and Hu [44]. The name of the method used and its limits of quantification for the analysed parameters were: Low Range (LR) reactor digestion and 3–150 mgCOD/L for COD, Nessler reagent and 0.02–2.5 mg NH_4^+-N/L for NH_4^+, High Range (HR) Cadmium reduction and 0.3–30 mgNO_3^- -N/L for NO_3^-, PhosVer 3 and 0.02–2.5 mgPO_4^{-3}/L for PO_4^{-3}, FerroVer and 0.002–3.00 mgFe/L for Total iron, and Nessler and 1–150 mgTKN/L for Total Kjeldahl Nitrogen. Excerpt for the pH measured using Orion Star A214 pH meter; other monitored parameters were analysed using DR 2800 spectrophotometer manufactured by HACH Company based in Berlin, Germany.

2.4. Statistical Analysis

The Microsoft Excel program was used in the statistical analysis of different data sets and plotting graphs. The statistical treatment of the results to determine the means, standard deviations, correlation coefficients, and significance were accomplished using Microsoft Excel 2019 software. The software was used to determine the statistical significance tests for some observations, $n > 10$, two-tailed student t-test, n–2 degrees of freedom, and the confidence interval, $p = 0.01$. The tests were performed to assess whether there was a significant difference in pollutants removal between (i) the systems with Fe^0 materials and the reference (system without Fe^0 materials) and (ii) the system with SI Fe^0 materials and that with SW Fe^0 materials. The Pearson correlation coefficient (R^2) was determined to evaluate the strength and direction of a linear relationship between the observed total iron and residual pollutants (COD, PO_4^{3-} and NO_3^- + NH_4^+) concentrations in the tested

Fe^0-supported anaerobic digestion systems. The adopted evaluation criteria were as follows: (i) the R^2 values >0.8 or <−0.8 depicts high positive or high negative correlation (ii) R^2 values from 0.6 to 0.8 or −0.6 to −0.8 depicts good positive or negative correlation (iii) R^2 values from 0.4 to 0.6 or −0.4 to −0.6 depicts moderate positive or negative correlation (iv) R^2 values from 0.2 to 0.4 or −0.2 to −0.4 depicts low positive or negative correlation, and (v) R^2 values between 0.2 and −2 fall in the no significant correlation [45].

The Design-Expert pro version 13 software was used to optimise metallic iron (Fe^0) materials dosages. The goal of optimisation in this study was to determine a dose (in mg/L) of Fe^0 materials that optimally minimises the observed concentrations of the pollutants (COD, PO_4^{-3} and $NO_3^- + NH_4^+$) in the Fe^0-supported anaerobic digestion of domestic sewage. The software was used to generate desirability indices to rank the performance of the tested anaerobic digestion systems. The indices are generated from several responses, factors, and goals. For this research, the responses were the observed COD, PO_4^{-3} and $NO_3^- + NH_4^+$ concentrations, the factors were time and Fe^0 materials dosages, and the goal was to minimise the pollutants' concentrations (COD, PO_4^{3-} and $NO_3^- + NH_4^+$). The indices range from zero outsides of the limits to one at the goal [46,47].

2.5. Determination of Pollutants' Removal Efficiency

The pollutants (COD, PO_4^{-3} and $NO_3^- + NH_4^+$) removal efficiency achieved in each reactor was calculated using the formula presented in Equation (1).

$$\eta = 100 \times (C_0 - C_t)/C_0 \tag{1}$$

where η = pollutants removal efficiency (%), C_0 = Initial pollutants concentration (mg/L), and C_t = pollutants concentration observed at any time (mg/L).

3. Results and Discussion

3.1. Fe^0 Reactivity

Figure 2 presents the observed iron concentration results resulting from SW and SI materials dissolution by 2 mM 1, 10 Phenanthroline. The results indicate that the observed iron concentrations increase with time and continuously increase even after 120 h of experimental operation. However, a linear increase was observed within 24 h of experimental operation. Similar observations were reported elsewhere [28]. The results indicate that higher iron concentration (7.11 mg-Fe/L) was attained with SW materials than that (3.7 mg-Fe/L) with SI materials within 120 h of experiment operation. Based on the procedures for specifying the Fe^0 materials' reactivity as adopted from Lufingo, Ndé-Tchoupé [30], the following results were obtained: (i) the identified linear (R^2 = 0.9786 for SI and R^2 = 0.9612 for SW) timeframe was between 2nd to 10th hour (Figure 2) (ii) the rate of dissolution (K_{phen}) for SI and SW materials were 4.41 μg/h and 5.05 μg/h, respectively (iii), amount of FeCPs (mg/L) on Fe^0 materials or the fraction thereof that is dissolved by 1, 10 Phenanthroline, b for SI and SW were 5.23 μg and 91.36 μg, respectively. Therefore, SW materials have a higher dissolution rate and are more reactive than SI materials. It is expected that SW will perform better than SI materials in the pollutants removal mechanisms that mainly depend on the reactivity of Fe^0 materials. However, too reactive Fe^0 materials (e.g., nano scaled Fe^0) have been linked with impairment of microbial degradation of pollutants, while lower reactive Fe^0 materials (e.g., micro-scaled Fe^0) with longer-lasting in anaerobic digestion, and slower release of the H_2 that support microbial respiration [48].

The two main reasons for the difference in reactivity among different Fe^0 materials are the surface area and the elemental composition (an alloy of iron and other metals) of the materials [28,49,50]. In this study, different percentages of heavy metals have been observed in the tested Fe^0 materials (Table 1). Although heavy metals have been reported to be inhibitory and toxic to some biochemical reactions in anaerobic digestions systems [51–53],

application of Fe^0 material reduces the concentrations of heavy metals in Fe^0-supported anaerobic digestion systems [54,55].
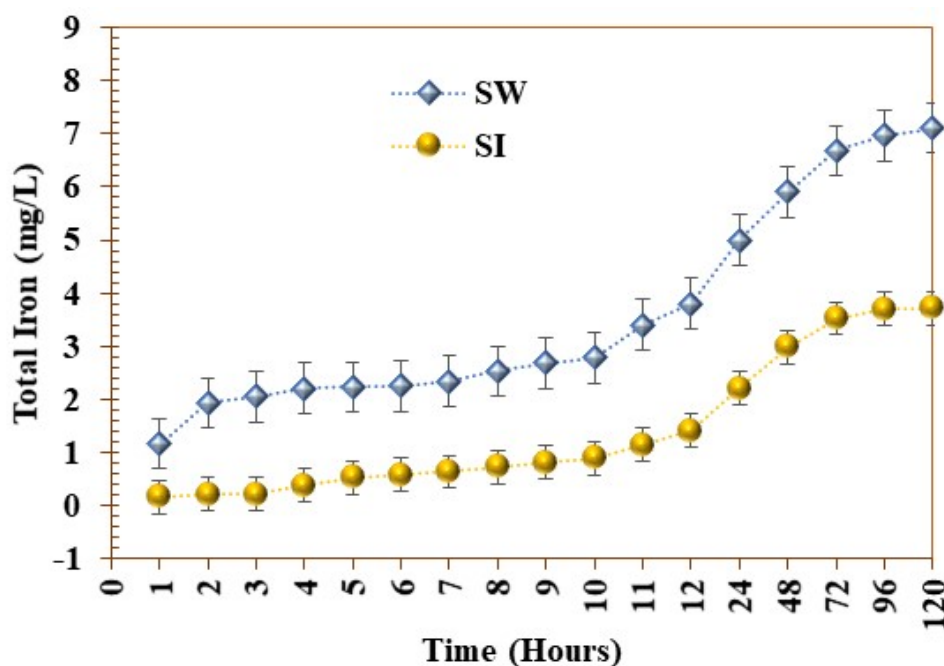

Figure 2. Comparison of iron dissolution by 2 mM 1, 10 Phenanthroline from SI and SW materials for 120 h. Experimental conditions: Mass of each Fe^0 = 0.1 g, Volume of working solution, V = 50 mL, room temperature, T = 37 ± 0.5 °C.

3.2. Effect of Fe^0 Materials Dosage on Pollutants Removal

3.2.1. COD

Figure 3a compares the COD removal efficiencies achieved due to the varied dosages of SI materials. The results show that the systems (II to VI) dosed with Fe^0 materials reached the stead state faster between 35th–39th days, in contrast with the system I (reference system) that attained the stead state two weeks later on the 53rd day of operation. Apart from that, the lowest (68.9%) and highest (87.7%) COD removal efficiencies were observed in systems I and IV, respectively (Figure 4).

Statistically, there was a significant difference in COD removal between System I (M = 42.3%, SD = 28.1%) and System IV (M = 63.2%, SD = 32.0%), t (31) = −10.4, $p < 0.01$, two-tailed. On the other hand, based on the maximum pollutant's removal efficiencies achieved (Figure 4) and the average observed COD concentrations (Table 3), the ranking of COD removal performance starting from the best to least performed system (among the systems dosed with SI materials) follows the following trend; IV > V > VI > III > II > I. The ranking shows the increased COD removal efficiency with the increased SI material dosages from 0 to 10 g/L and the decreasing COD removal efficiencies for the SI dosages above 10 mg/L (15 and 30 g/L).

The improved performance of anaerobic digestion of wastewater by Fe^0 materials addition has been reported in different studies. For instance, it was reported that Fe^0 materials facilitate fermentation, provide a more favourable environment for anaerobic digestion, accelerate hydrolysis and fermentation stages, cause proliferation of microbes [12,19,20]. On the other hand, the decrease in pollutants removal efficiency noted at higher dosages (15 and 30 g/L) of Fe^0 materials (Figures 3a and 4) may be due to negative impacts by higher SI dosages, as reported elsewhere [12,41]. Antwi [41] reported the following findings when studied the impact of Fe^0 dosing on biomethanation and distribution of microbial community in Fe^0-supported AD: (i) the microbial community population was optimally enhanced at 10 g/L dosage of Fe^0 and (ii) depopulation of the microbes was significant at

higher dose (20 g/L) of Fe^0 materials. According to Wu [12], higher Fe^0 dosages negatively impact the microbial activities in anaerobic digestion through encapsulation and damage of the cells' structures. However, among the tested dosages (3, 7, 15, 25, and 50 g/L) of Fe^0 powder in swine wastewater treatment, the negative effects were observed in Fe^0 dosage of 50 g/L [12]. While in this research, the effects were observed in 15 and 30 g/L dosages. According to Konadu-Amoah [56], the addition of Fe^0 materials into the polluted water lead to a generation of iron corrosion products (FeCPs) that mediate contaminants removal. However, excessive precipitating FeCPs (Equation (3)) due to higher Fe^0 materials doses may enmesh, adsorb and or inactivate some microorganisms responsible for the digestion of the pollutants [56–58]. Although the increased Fe^0 materials mass loading is required for producing enough H_2 for the microbial respiration (Equation (2)) [13,20,48] but too large doses should be avoided for contra-productivity, as shown here (Figure 3a and Table 3) and elsewhere [12,18]. Therefore, the case-to-case optimisation studies for Fe^0 materials dosage must be carried out because the effects of the materials in the anaerobic digestion of wastes may significantly vary with the nature of the treated wastes and or type and dosage of Fe^0 materials.
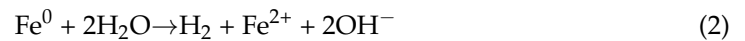
$$Fe^0 + 2H_2O \rightarrow H_2 + Fe^{2+} + 2OH^- \tag{2}$$

$$Fe^{3+} + Fe^{2+} + nH_2O \rightarrow Fe^{II}, Fe^{III} \text{ and mixed oxyhydroxides} \tag{3}$$

Table 3. Residual pollutants concentration in the systems. Experiments were operated at $37 \pm 0.5\ °C$ for 76 days. Avrg stands for average, and S.D for standard deviation.

| System | Parameters | | | | | | | | | |
| | COD (mg COD/L) | | $NO_3^- + NH_4^+$ (mg NO_3^- + NH_4^+/L) | | PO_4^{3-} (mg PO_4^{3-}/L) | | Total-Fe (mg Fe/L) | | pH | |
	Avrg	S.D	Avrg	S.D	Avrg	S.D	Avrg	S.D	Avrg	S.D
I	235	115	89.1	8.6	19.21	2.96	0.53	0.25	7.01	0.16
II	177	120	79.7	5.6	15.62	4.40	1.38	0.29	7.05	0.12
III	166	124	73.8	6.1	10.70	5.26	2.19	0.87	7.09	0.12
IV	150	130	62.0	11.4	4.53	6.26	3.99	1.62	7.38	0.15
V	153	128	68.3	10.4	7.83	6.03	3.18	1.70	7.22	0.13
VI	159	125	69.9	8.54	9.74	5.83	2.52	1.02	7.18	0.14

3.2.2. PO_4^{3-}

Figure 3b compares the PO_4^{3-} removal efficiencies achieved due to the varied dosages of SI materials. The impact of the varied dosages of SI materials on the removal of orthophosphate achieved in the reactors was evaluated based on the removal efficiencies. Ranking of the reactors' performances based on the maximum PO_4^{3-} removal efficiencies (Figure 4) and the average observed PO_4^{3-} concentrations (Table 3) starting from the best to least performed system (among the systems dosed with SI materials) follows the following trend; IV > V > VI > III > II > I. The lowest (7.3%) and highest (98.3%) PO_4^{3-} removal efficiencies were observed in 0 g/L and 10 g/L reactors, respectively (Figure 4). Statistically, there was a significant difference in PO_4^{3-} removal between System I (M = 7.9%, SD = 16.6%) and System IV (M = 74.5%, SD = 35.2%), t (31) = −20.1, $p < 0.01$, two-tailed.
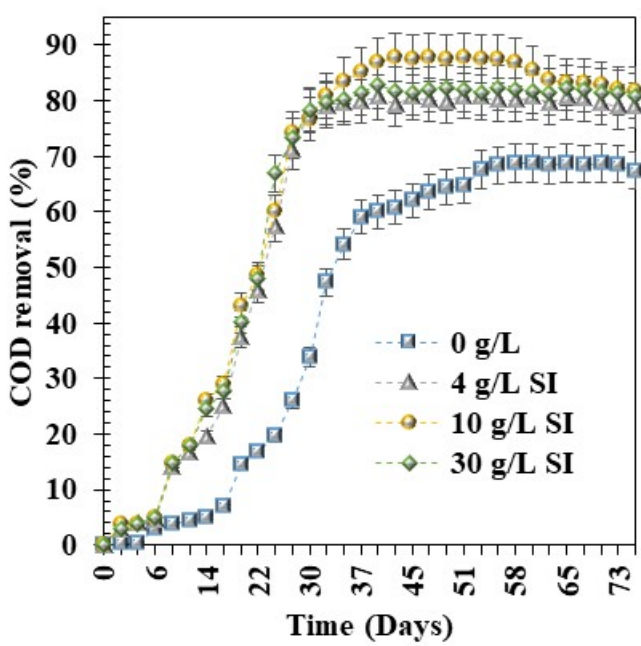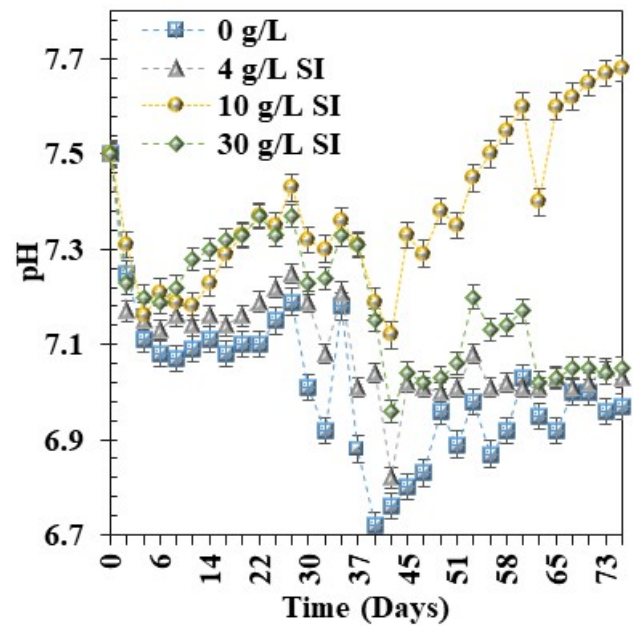
(**a**)
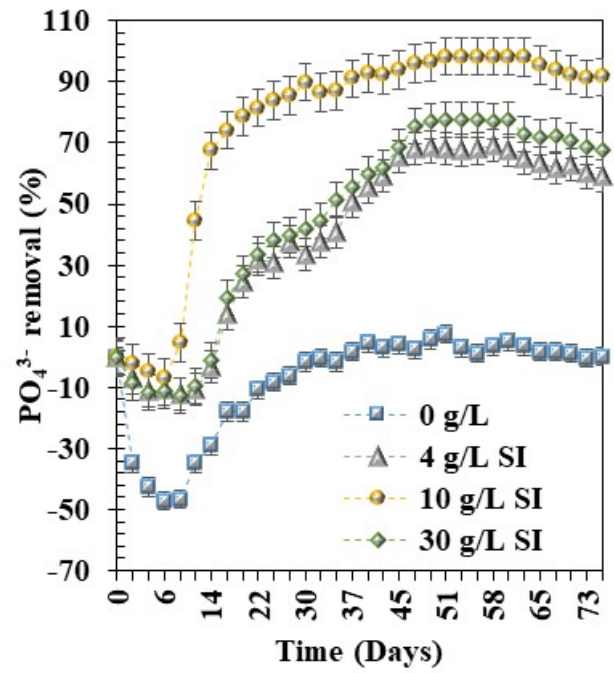
(**b**)
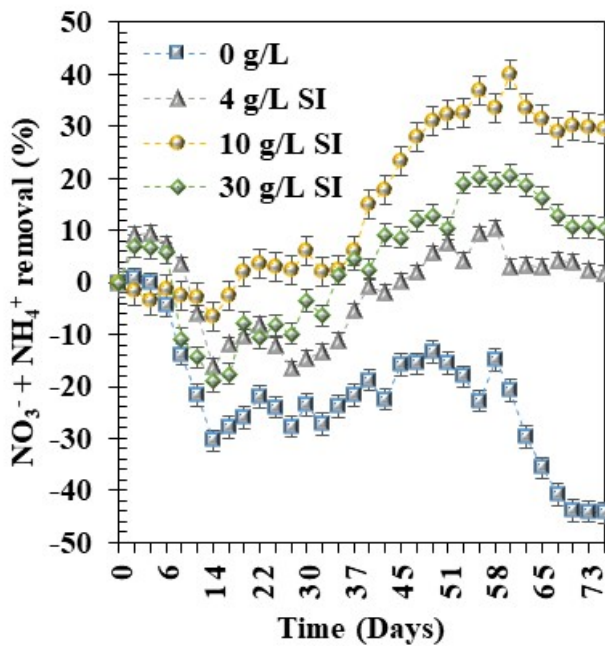
(**c**)

(**d**)

Figure 3. Comparison of the effects of varying SI materials dosages in pollutants removal efficiency. (**a**) COD removal; (**b**) PO_4^{3-} removal; (**c**) $NO_3^- + NH_4^+$ removal; (**d**) pH variations. SI materials' dosages were 0 g, 4g/L, 10 g/L, 15 g/L and 30 g/L; Systems' temperature, T = 37 ± 0.5 °C.
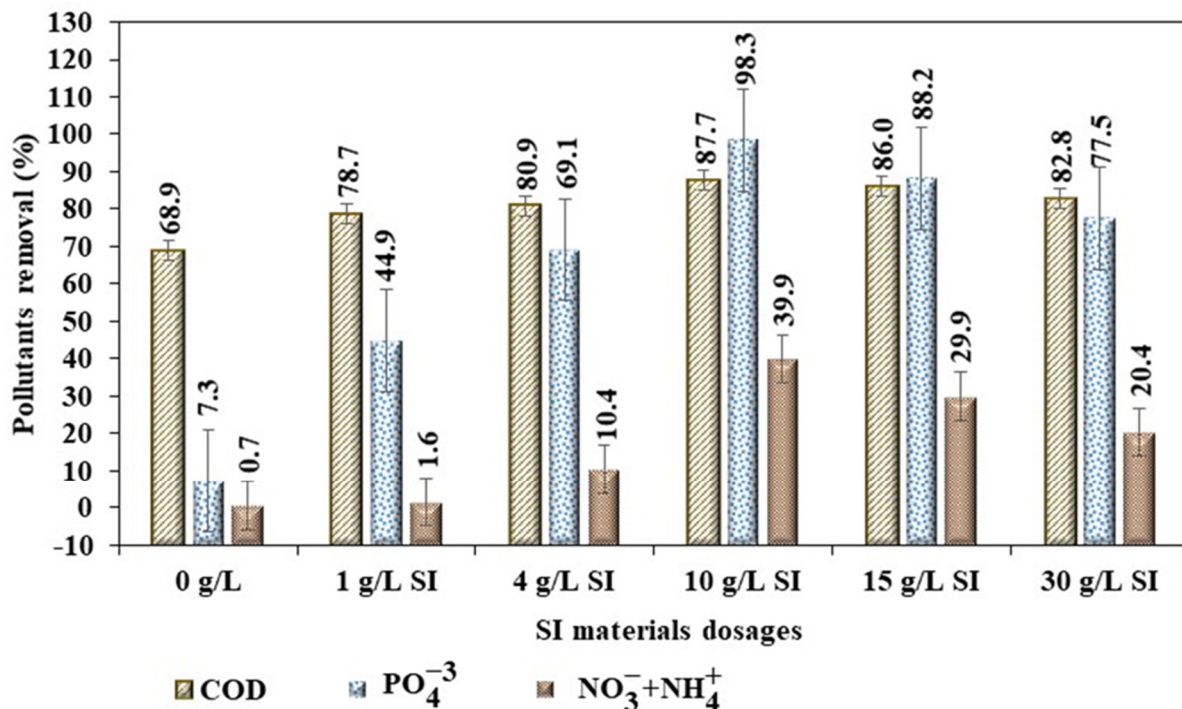
Figure 4. Comparison of maximum pollutants removal efficiencies among systems. SI materials' dosages were 0 g, 4g/L, 10 g/L, 15 g/L and 30 g/L; Systems' temperature, T = 37 ± 0.5 °C.

The trend of the observed removal of orthophosphate in the reactors is presented in Figure 3b. The increasing trend of orthophosphates concentration in the reactors in the initial eight days of the start-up period may be mainly linked to the partitioning of the soluble phosphorus between the solid (from the seed sludge and domestic sewage) and liquid phases influenced by pH and temperature changes. Drop in pH and rise in temperature contribute to the dissolution of the bound phosphorus. During this period: (i) within 22 min, the temperatures of the reactors' contents were raised from 24 °C to a constant operational temperature of 37 ± 0.5 °C in a water bath (ii) the pH dropped in all reactors (Figure 3d) (iii) the highest increase in PO_4^3 concentration from 17.8 to 26.1 mg/L (Figure 3b) and the highest drop in pH from 7.5 to 7.1 was observed in the System I (Figure 3d) and (iv) the observed PO_4^{3-} concentration in the System I is negatively related to pH with a correlation coefficient, $R^2 = -0.99$. Previous studies also linked rising concentration of soluble phosphates in anaerobic digestion with the hydrolysis of the bound phosphorus and dissolution of the same in low pH values [59,60]. The decrease in PO_4^{3-} concentration observed from the second week of operation (Figure 3b) for the reference reactor is possibly due to microbial removal through cell synthesis [6] and precipitation by cations (Ca^{2+} and Mg^{2+}, Al^{3+} and Fe^{2+}) that usually present in wastewaters or adsorption by suspended solids [59,61,62]. Although this study did not monitor all the cations, the maximum total iron concentration of 1.09 mg/L was observed in the reactor without Fe^0 materials.

Results presented in Figure 4 show that the lowest (7.3%) and highest (98.3%) PO_4^{3-} removals were achieved in the reference reactor (System I) and System IV, respectively. The results imply that Fe^0 materials increased the overall performance of the anaerobic system in PO_4^{3-} removal by more than 90%. Low PO_4^{3-} removal is known in conventional anaerobic wastewater treatment. For instance, the overall phosphorus removal of less than 10% has been reported in full-scale anaerobic digestion plants [63]. The higher PO_4^{3-} removal achieved in reactors dosed with SI materials (Figure 4) is conceivably due to enhanced precipitation and adsorption of phosphorus by the Fe^0 materials corrosion products. The removal of phosphate by metallic iron can be realised through adsorption by hydrous

ferric, phosphate incorporation into the structure of hydrous oxide, and formation of ferric phosphates as generally described by Equation (4) [6,32,64].

$$1.6Fe^{3+} + H_2PO_4^- + 3.8OH^- \xrightarrow{pK = 67.2} Fe_{1.6}H_2PO_4(OH)_{3.8}\downarrow \tag{4}$$
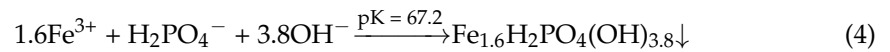
On the other hand, it was expected for the higher Fe^0 dosages (i.e., 15 and 30 g Fe^0/L) to perform better in PO_4^{3-} removal because of proportional increases of active sites with the increase of Fe^0 dosages (linear relationship) [29]. However, due to the complexity of the Fe^0-mediated biological pollutants removal systems, nonlinear relationships have also been reported [30]. For instance, in the fluidized Fe^0 bed reactor for nitrate removal, the nitrates concentrations remained constant for the Fe^0 dosages greater than 10 g [40]. The relatively lower performance of higher dosages of Fe^0 materials in this study is perhaps due to the following: (i) less bioaccumulation of phosphorus due to fewer microbes in the systems with higher Fe^0 dosages (Section 3.2.1) (ii) the rapid precipitation of the FeCPs may quickly form a layer that blocks the mass transfer of pollutant (PO_4^{3-}) between Fe^0 materials at the bottom of the reactor and the pollutants in the solution (domestic sewage) (Section 3.2.1). The inactivation by FeCPs is expected to be more severe in this study because the reactors were operated in batch mode without mixing [29,30].

3.2.3. $NO_3^- + NH_4^+$

Figure 3c compares the effects of the varied dosages of SI materials on removing $NO_3^- + NH_4^+$. The results show a general increasing trend of $NO_3^- + NH_4^+$ concentration in all the reactors for the first two weeks of operation followed by a continuous decrease for the next six weeks, and back to the increasing trend for the rest three weeks of operation. Ranking of $NO_3^- + NH_4^+$ removal performance (among the systems dosed with SI materials) starting from the best to least performed system follows the following trend; IV > V > VI > III > II > I (Figure 4 and Table 3). The lowest (0.7%) and highest (39.9%) $NO_3^- + NH_4^+$ removal efficiencies were observed in System I and System IV, respectively (Figure 4). Statistically, there was a significant difference in $NO_3^- + NH_4^+$ removal between System I (M = −22.2%, SD = 11.9%) and System IV (M = 14.9%, SD = 15.7%), t (31) = −5.2, *p* < 0.01, two-tailed.

According to Till [23], the abiotic reactors fed with steel wool converted the entire added nitrate to ammonium (Equation (5)) while the biotic reactor fed with the same materials caused more denitrification (Equation (6)) than the generation of ammonium. The results imply that the Fe^0 materials in the reactors without microbes convert nitrogen to ammonium, while with the presence of microbes, the materials cause more denitrification than the production of ammonium. Therefore, based on these findings, the increase in $NO_3^- + NH_4^+$ concentration observed during the initial stages of the reactors' operation was due to relatively fewer denitrifying bacteria and, therefore, a more significant portion of the nitrogen converted to ammonium.

On the other hand, the observed decreasing of $NO_3^- + NH_4^+$ concentration in the reactors may be associated with the build-up of denitrifying bacteria population that denitrified most of the available nitrogen. The relatively high performance of Fe^0 materials dosed reactors compared to the reference reactor can be linked to the proliferation of microbial community due to enhanced hydrogen respiration by the Fe^0 materials [13,20]. According to Deng [13], Fe^0 materials enriches autotrophic denitrifiers.

$$4Fe^0 + NO_3^- + 7H_2O \rightarrow 4Fe^{2+} + NH_4^+ + 10OH^- \tag{5}$$

$$2NO_3^- + 5H_2 \rightarrow N_2 + 4H_2O + 2OH^- \tag{6}$$

The decrease in $NO_3^- + NH_4^+$ removal efficiency noted at higher dosages (15 and 30 g/L) of Fe^0 materials (Figures 3c and 4) may be due to inactivation and depopulation of the nitrifiers caused by higher Fe^0 dosages as elaborated in Section 3.2.2. Specifically, the inactivation and death of the denitrifiers have been reported by Schädler [65]. The

report describes that FeCPs adsorbs and form a layer to the cells' surfaces of microbes that interfere with substrate and nutrients diffusion to the cell, consequently leading to the stagnation and, eventually, the death of the microbes.

The decline in $NO_3^- + NH_4^+$ removal from around 45th day of operation (Figure 3c) is conceivably a result of higher death rate of cells than production due to substrate deficit [5,6]. Therefore, the increase in nitrogen concentration in the system is presumably due to release by the decomposed dead cells. It is also perceived that the nitrate from the decomposition of the dead microbes is converted more to ammonium by Fe^0 than denitrified because of the negligible number of microbes as described elsewhere [23].

3.3. Effects of Types of Fe^0 Materials on Pollutants Removal

Figure 5a compares the impact of different types of Fe^0 materials on COD removal. Generally, the figure indicates that compared to the reactor without Fe^0 materials, both SI and SW materials improved the performance of the reactors to remove COD. However, statistically, there was no distinguishable difference in the observed COD removal between System IV (M = 63.2%, SD = 32.0%) and System VII (M = 63.5%, SD = 31.9%), t (31) = −1.2, $p > 0.01$, two-tailed. Therefore, based on the statistical analysis, similar results are expected when either SI or SW materials are applied in Fe^0-supported anaerobic digestion of domestic sewage for COD removal.

Results in Figure 5b describes the comparison of the impact of SI and SW materials on PO_4^{3-} removal. The results indicate that the PO_4^{3-} removal in all observations were lower in the reference (System I) than in System IV or VII. Therefore, compared to the reference, both SI and SW materials improved the performance of the reactors in removing PO_4^{3-}. However, statistically, there was a significant difference in PO_4^{3-} removal between System IV (M = 74.5%, SD = 35.2%) and System VII (M = 87.1%, SD = 27.1%), t (31) = −3.5, $p < 0.01$, two-tailed. The statistics show that SW materials will perform better than SI materials in Fe^0-supported anaerobic digestion of domestic sewage for PO_4^{3-} removal. Since the PO_4^{3-} removal is mainly due to enhanced precipitation and adsorption of phosphorus by the Fe^0 materials corrosion products. The results were expected because the tested SW materials have a higher dissolution rate than scrap iron materials (Section 3.1). The higher reactivity of SW compared to SI materials results in more generation FeCPs that scavenge and remove more PO_4^{3-} (Section 3.2.2). It was expected that the remarkable raising of pH observed in system VII from around 45th day of the reactors operation (Figure 5d) could significantly affect the removal of PO_4^{3-} because at higher pH values passivation of Fe^0 materials by FeCPs is high [66]. However, the expected pH raising effects could not be evident probably because the Fe^0 materials performance was already affected by passivation caused by aging as reported elsewhere [67].

Comparison of the impact of SI and SW materials on the removal of nutrients as $NO_3^- + NH_4^+$ is presented in Figure 5c. The results show that the minimum observed $NO_3^- + NH_4^+$ removal in all observations were relatively lower in the reference (System I) than in System IV or VII. Accordingly, compared to the reference, both SI and SW materials improved the performance of the reactors in removing $NO_3^- + NH_4^+$. However, statistically, there was no distinguishable difference in the observed $NO_3^- + NH_4^+$ removal between 10 g/L SI reactor (M = 14.9%, SD = 15.7%) and 10 g/L SW reactor (M = 12.1%, SD = 9.8%), t (31) = 1.6, $p > 0.01$, two-tailed. Although Fe^0 significantly improved the removal of $NO_3^- + NH_4^+$ as compared to the system without Fe^0 (Section 3.2.3), $NO_3^- + NH_4^+$ was the least removed pollutant (among COD, $NO_3^- + NH_4^+$ and PO_4^{3-}) regardless the type of Fe^0 materials used (Figure 5a–c). The less removal of the pollutant is conceivable because some nitrate present in the system is converted to ammonium instead of denitrification (Section 3.2.3). Within four (4) days of reactors' operation, the observed NH_4^+ and NO_3^- removals were; −4.1% and 4.0% for the system I, −17.1% and 33.3% for system IV, and −18.6% and 58.1% for system VII. During this period of reactors' operation, it was clear that there was a relatively higher; (i) nitrate removal in the reactors dosed with Fe^0 materials compared with the reference system (system I) (ii) NH_4^+ accumula-

tion rate in the reactors dosed with Fe^0 materials compared with the reference system (iii) NO_3^- removal in the reactor dosed with SW materials (system VII) compared to that with SI materials (system IV) (iv) NH_4^+ accumulation rate in the reactor dosed with SW materials compared to that with SI materials. The relatively higher NO_3^- removal and NH_4^+ accumulation rates in the Fe^0 materials dosed reactors (systems IV and VII) compared to the reference (System I) may be linked to the conversion of some NO_3^- to NH_4^+ instead of denitrification (Section 3.2.3). The relatively higher NO_3^- removal and NH_4^+ accumulation rates in System VII compared to System IV may be linked to the higher reactivity of SW materials in System VII (Section 3.1). The relatively higher removal efficiency decline rate of NO_3^- + NH_4^+ as from 45th day for 10 g/L SW (Figure 5c) may be attributed to the higher death rate of microbes resulting from substrate deficit and abrupt rise in pH. The suitable pH range for anaerobic wastewater treatment is 6.5 to 7.8, and above the pH of 8.5, ammonia toxicity to the methanogens begins [64]. Therefore, it is perceived that the decomposing biomass of the dead microorganisms release the nitrogen.
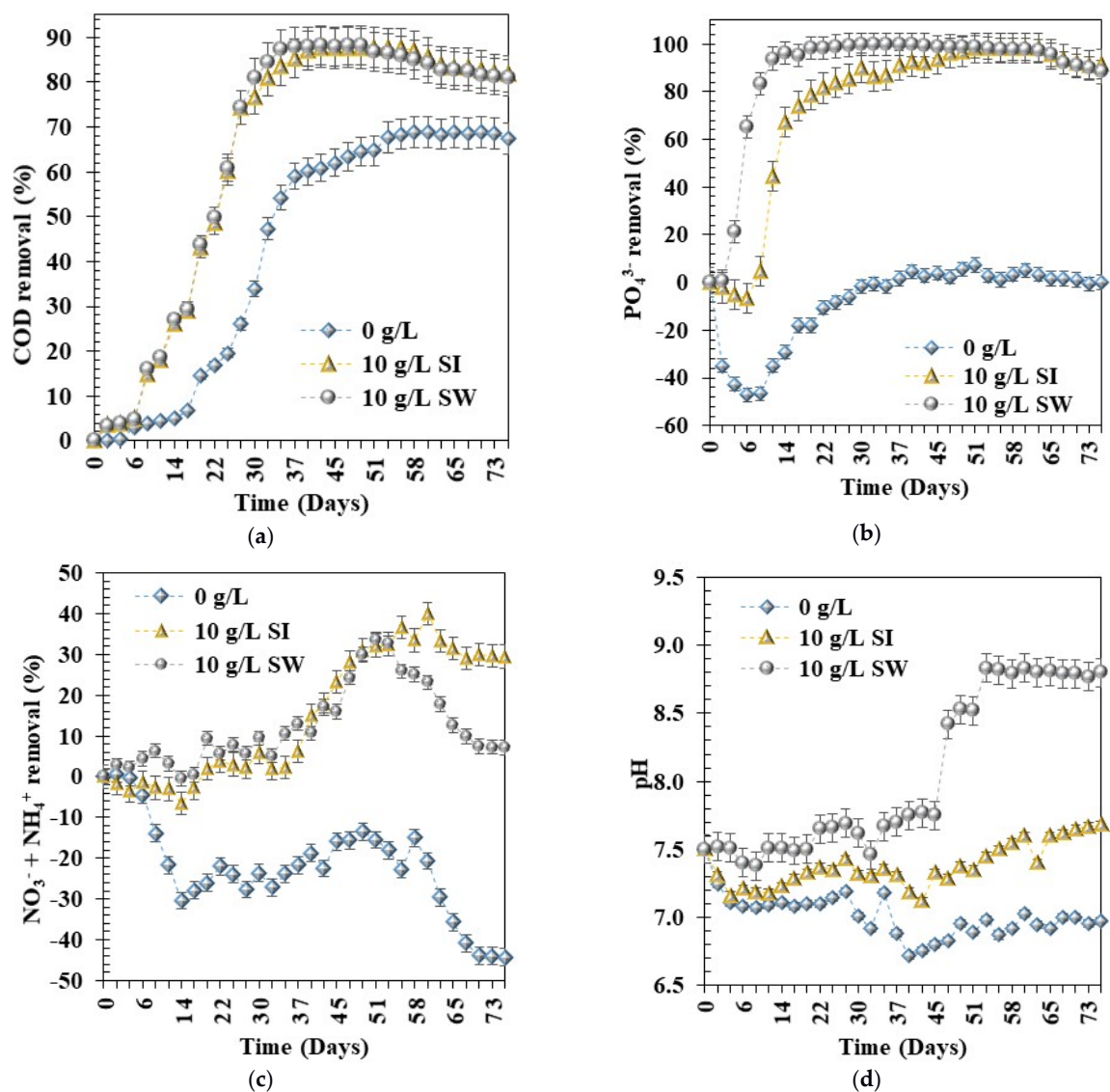

Figure 5. Comparison between SI and SW materials' effect on pollutants removal (**a**) COD removal; (**b**) PO_4^{3-} removal; (**c**) NO_3^- + NH_4^+ removal; (**d**) pH variations. Fe^0 materials' dosages were 0 g, 10 g/L SI, and 10 g/L SW; Systems' temperature, T = 37 ± 0.5 °C.

Statistical analysis shows negative relationships between the observed pollutants (COD, NO_3^- + NH_4^+, and PO_4^{-3}) and total iron concentrations in Systems IV and VII.

The correlation coefficients between the observed pollutants and total iron concentrations for System IV were; $R^2 = -0.93$ for COD, $R^2 = -0.90$ for PO_4^{3-}, and $R^2 = -0.21$ for $NO_3^- + NH_4^+$ while for System VII were; $R^2 = -0.78$ for COD, $R^2 = -0.86$ for PO_4^{3-}, and $R^2 = -0.45$ for $NO_3^- + NH_4^+$. The results imply that the higher the dissolution of Fe^0 materials, the higher is the removal of pollutants (COD, $NO_3^- + NH_4^+$, and PO_4^{3-}). Regarding that, it was expected that the tested SW materials with a higher dissolution rate than scrap iron materials (Section 3.2) to perform significantly better in the removal of all analysed pollutants (COD, $NO_3^- + NH_4^+$, and PO_4^{3-}), but it was not particularly for COD and $NO_3^- + NH_4^+$. The reason may be because the removal of COD and $NO_3^- + NH_4^+$ is highly dependent on microbial digestion, in contrast with the PO_4^{3-} removal, which mainly depends on the enhanced precipitation and adsorption by the Fe^0 corrosion products. However, the correlation coefficient $R^2 = -0.21$ for $NO_3^- + NH_4^+$ implies that there is low negative correlation between the observed $NO_3^- + NH_4^+$ and total iron concentrations (Section 2.4). Therefore, $NO_3^- + NH_4^+$ removal is not strongly dependent on the increase of the total iron concentration in the system. The reason may be because excessive iron concentrations may abiotically convert NO_3^- to NH_4^+ instead of the desired denitrification (Section 3.2.3).

The SW materials raised the pH of domestic sewage above recommended range for anaerobic digestion. The suitable pH range for anaerobic wastewater treatment is 6.5 to 7.8, and above the pH of 8.5, ammonia toxicity to the methanogens begins [61,64]. However, the following ranges in pH changes were observed: 7.5 to 6.7 in System I, 7.5 to 7.7 in System IV and 7.5 to 8.8 in System VII (Figure 5d). Therefore, the results suggest that: (i) Fe^0 materials have the potential to raise the pH of domestic sewage, and (ii) SW materials have a higher chance than SI to cause the problem of high pH in Fe^0-supported anaerobic digestion of domestic sewage. Different research in different types of wastewaters also have reported different pH rise ranges caused by the addition of Fe^0 materials. For instance, in Fe^0 aided anaerobic treatment of pome oil mill effluent, the pH range between 7–9 was observed [16]. The potential of Fe^0 materials to raise the pH in anaerobic digestion can be linked to hydroxyl ions released during anaerobic oxidation of the materials (Equation (2)). Similarly, according to [21], steel wool Fe^0 materials with a small specific area did not significantly raise the pH in the anaerobic digestion of synthetic wastewater, while the Fe^0 powder with a relatively larger specific area raised the pH of the wastewater to above 10. The case possibly is the reason in this study that the SW materials caused a relatively higher rise in the pH of domestic sewage than SI materials. The rising of pH observed in system VII from around 45th day of the reactors operation (Figure 5d) was perhaps due to depletion of volatile fatty acids that served as a pH buffer [43]. The pH effect was significant in system VII, perhaps because of the higher reactivity of SW compared to SI materials leading to more generation of hydroxyl ions (Equation (2)).

3.4. Optimisation of Fe^0 Materials Dosage

The optimum dosage of the studied materials was analysed to minimise the concentration of pollutants (COD, $NO_3^- + NH_4^+$ and PO_4^{3-}) in the treated effluents. The summary of optimisation constraints is presented in Table 4. Furthermore, Table 5 summarises the optimum solutions of the objective function based on the highest desirability index for each of the tested dosages of Fe^0 materials.

The performance ranking of systems based on simultaneous removal of pollutants (COD, $NO_3^- + NH_4^+$ and PO_4^{-3}) are presented in terms of desirability indices in Table 5. The ranking followed the following trend; IV > VII > V > VI > III > II > I. The optimum system (System IV) scored the highest desirability index of 0.985. The remained COD, $NO_3^- + NH_4^+$ and PO_4^{-3} concentrations in the optimum reactor were 57.9 mg COD/L, 43.8 mg $NO_3^- + NH_4^+$/L, and 0.5 mg PO_4^{3-}/L, respectively, attained within 60 days of operation (Table 5).

Table 4. Set of constraints for optimisation of the objective function.

Name	Goal	Lower Limit	Upper Limit	Lower Weight	Upper Weight	Importance
A: Time	is in range	0 days	76 days	1	1	3
B: Fe^0 Dosage	is in range	0 g Fe^0/L	30 g Fe^0/L	1	1	3
COD	minimise	48 mg COD/L	408 mg COD/L	1	1	3
PO_4^{-3}	minimise	0.3 mg PO_4^{3-}/L	26.2 mg PO_4^{3-}/L	1	1	3
$NO_3^- + NH_4^+$	minimise	43.8 mg NO_3^- + NH_4^+/L	105.2 mg NO_3^- + NH_4^+/L	1	1	3

Table 5. Ranking of systems performance based on desirability indices. Avrg stands for average, and S.D for standard deviation.

Time (Days)	System	COD (mg COD/L)		PO_4^{3-} (mg PO_4^{3-}/L)		NO_3^- + NH_4^+ (mg NO_3^- + NH_4^+/L)		Desirability
		Avrg	S.D	Avrg	S.D	(mg/L)	S.D	
60	IV	57.9	3.2	0.5	0.1	43.8	10.4	0.985
53	VII	54.5	3.2	0.3	0.5	54.6	4.5	0.932
53	V	56.7	3.1	3.6	0.4	50.8	9.6	0.907
51	VI	65.3	3.1	6.7	0.7	52.5	9.8	0.848
58	III	66.1	3.0	6.3	0.6	65.3	6.0	0.777
58	II	81.2	3.0	11.4	1.1	71.7	5.7	0.654
49	I	142.3	2.8	15.4	1.5	82.7	9.0	0.482

3.5. Behaviour of Fe^0 Materials in Domestic Sewage

Figure 6a,b presents the comparison of the potentials of different Fe^0 materials (SI and SW) to raise pH of the different mediums (domestic sewage and distilled water).

A relatively higher maximum pH values (9.4) was observed in System IX compared to that (8.8) in System VIII (Figure 6a). On the other hand, a relatively higher maximum pH value (8.8) was observed in System VII compared to that (7.5) in System IV (Figure 6b). Apart from that, the observed pH of distilled water in System IX raised to a maximum value (9.4) within six days of operation (Figure 6a), while that of domestic sewage in System VII was raised to the maximum value (8.8) within sixty days of operation (Figure 6b). Therefore, the results suggest that: (i) SW has a higher potential in raising the pH of both water and domestic sewage than SI materials and (ii) Fe^0 materials raise the pH of distilled water faster than domestic sewage. Anaerobic digestion of wastewater goes through the acidogenesis stage marked with the generation of volatile fatty acids, particularly butyrate, propionate, and valerate [6]. Therefore, a portion of OH^- released during anaerobic oxidation of Fe^0 materials (Equation (2)) is neutralised; hence the system's pH is regulated.

Results on the impact of SI and SW materials on the observed total iron concentration in the reactors fed with the same domestic sewage or distilled water are presented in Figure 6c,d. The results indicate that the maximum total iron concentrations in Systems IV, VII, VIII, and IX were 6.19 mg/L, 7.05 mg/L, 7.70 mg/L, and 10.80 mg/L, respectively. The results imply that the dissolution of SW material is higher than that of SI materials in both domestic sewage and distilled water. The observed total iron concentration dropped sharply from maximum to the lower minimum in distilled water (Figure 6c) compared to in domestic sewage (Figure 6d). The phenomenon occurs because the passivation rate of metallic iron materials reduces in the presence of organic carbon [13]. The organic carbon content in distilled water is certainly negligible compared to domestic sewage. The higher decreasing rate of the total iron concentration observed in system VII compared to system

IV from around the 45th day of the reactors' operation (Figure 6d) was perhaps due to the higher passivation rate of SW materials caused by the rise in pH (Figure 5d) in system VII compared to IV. The passivation rate of Fe^0 by FeCPs is higher in alkaline condition [68].
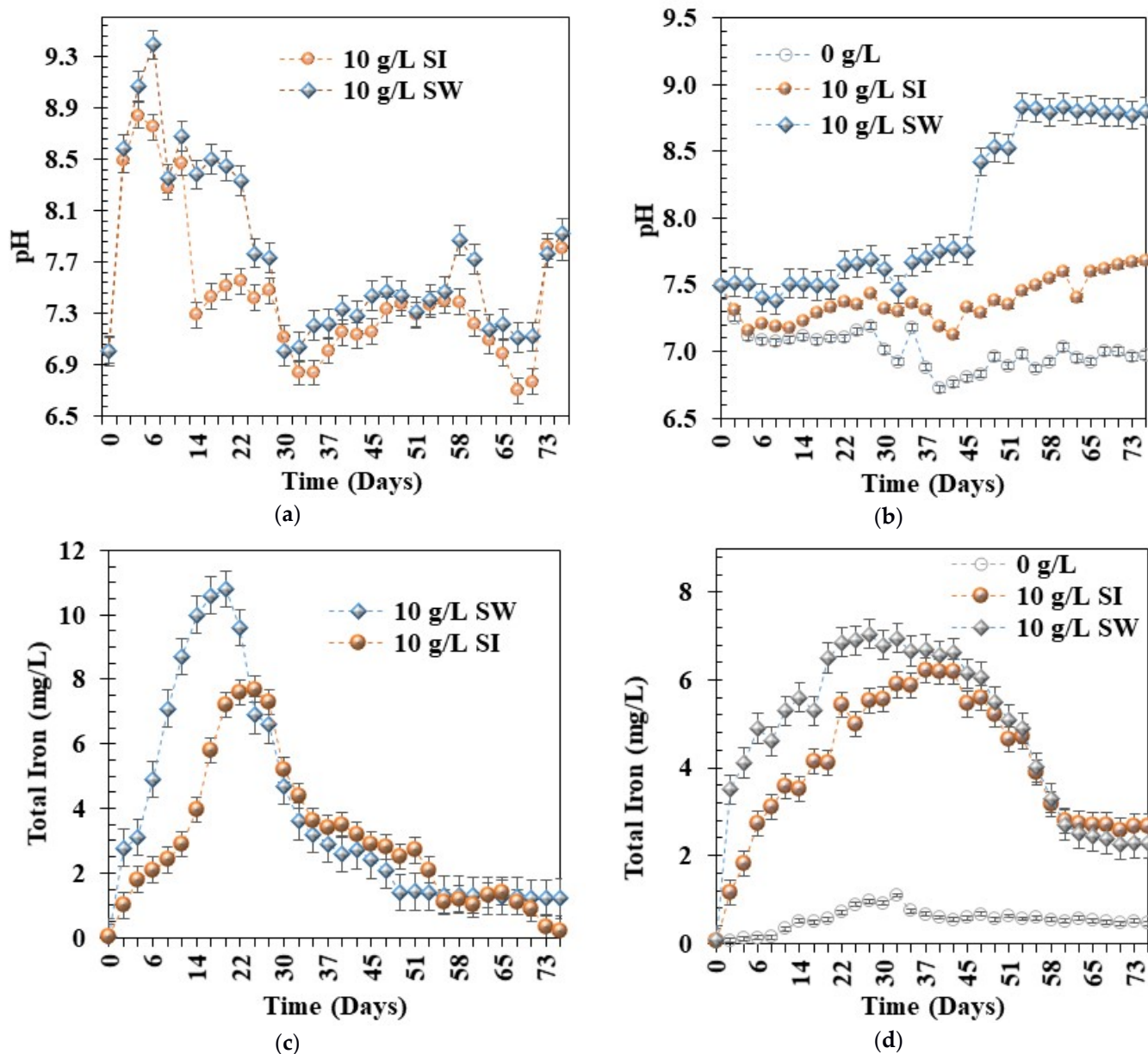

Figure 6. pH and total iron concentration variations resulting from 10 g/L of Fe^0 materials (SW or SI) dosage in distilled water or domestic sewage. (**a**,**c**) Fe^0 materials in distilled water; (**b**,**d**) Fe^0 materials in domestic sewage. Systems' temperature, T = 37 ± 0.5 °C.

3.6. Significance of the Results

This study shows that under the stated experimental conditions ($0 \leq [Fe^0]$ (g/L) ≤ 10, for scrap iron), "cathodic H_2" [23] from Fe^0 oxidation by water (Equation (2)) is highly effective in improving the performance of anaerobic digestion systems for the removal of organics from domestic sewage. Since the proof of concept in 1998 by Till [23] using nitrate as probe substance, an impressive body of research has been devoted to extend the application of Fe^0-supported anaerobic digestion to wastewater treatment [22,69–73] and biogas production [22,74–76]. However, related investigations were mostly designed and performed on a pragmatic case-to-case basis [31,77]. In particular, it has not been properly considered that each Fe^0 material reacts differently in a given Fe^0/water system (Section 3.1,

Figure 2) [28]. In fact, all Fe^0 specimens have the same electrode potential $E^0 = -0.44$ V. Therefore, reported improving or inhibiting effects of the presence of Fe^0 on the efficiency of anaerobic digestors are due to differences in the kinetics of the reaction after Equation (2) (H_2 generation) and associated reaction (Equation (3)) (scavenger of microorganisms) under actual operational conditions. It is important to recall that scrap iron (SI) and steel wool (SW) are not homogeneous classes of Fe^0 materials [28,78–80]. For example, there exist 7 classes of Fe^0 SW with differentiated reactivity [28,80].

When H_2 is generated at the Fe^0 surface, it is transported by diffusion across the oxide scale into the bulk solution where it initiates microbial activities for the degradation of organics. The extent of related processes depends on the solution chemistry (e.g., pH value) and the availability of nutrients (NO_3^-, PO_4^{3-}) [23,70]. In other words, there is no stoichiometric relationship between the level of H_2 generated (Equation (2)) and the extent of contaminant degradation. Conversely, the removal of contaminants by solid iron corrosion products (FeCPs) and their hypothetical degradation by electrons from Fe^0 [81] are related to some stoichiometry [82–85]. Accordingly, higher Fe^0 levels in a system implies the in-situ generation of more FeCPs which are excellent scavengers of micro-pollutants and microorganisms, including pathogens [86,87]. As Fe^0 corrodes, FeCPs is continuously generated and acts as microorganism scavengers. In other words, the growth of microorganisms is inhibited. As the corrosion rate declines [88], less FeCPs is generated and more microorganisms survive. When the rate of FeCP precipitation becomes significantly lower than the rate of microorganism generation, the extent of degradation of organics increases. It is thus not surprising, that for the initial phase of the operation a lag time is observed before biodegradation is quantitative [89]. This lag time is prolonged with higher Fe^0 loadings (Figure 6). Therefore, designing non-site-specific Fe^0-supported anaerobic digestors for wastewater treatment is an almost impossible task. However, if a significant body of data exists on treatment rates for a wastewater type using different Fe^0 materials, site-specific treatability studies will be only required to fine-tune design criteria for the optimal performance of the system.

By demonstrating that the efficiency of Fe^0-supported anaerobic digestors for wastewater treatment depends primarily (but not exclusively) on the amount of FeCPs in the system, this study provides a clear starting point for the design of future laboratory, pilot, and field-scale studies. Further work is required to explore relevant limiting factors for efficient Fe^0-supported anaerobic digestors including Fe^0 loading, Fe^0 size, Fe^0 type, mass transfer effects, reactor volume, and reaction time [77,90]. This would have sizing, and therefore, economic implications for digestor design.

4. Conclusions

This research reveals that Fe^0 materials significantly improve the performance of anaerobic systems to remove organics and nutrients simultaneously. The minimum residual COD (50 mg/L), $NO_3^- + NH_4^+$ (43.8 mg/L), and PO_4^{3-} (0.3 mg/L) concentrations were observed in the optimally performed reactor (System IV). The observed quality of the effluent for COD is similar to that from conventional activated sludge system (45–120 mg/L) and far better than that from the UASB and Maturation Ponds (100–180 mg/L) [91]. Although, according to Riffat [5] removing nutrients by the anaerobic secondary system may be difficult, this research presents the possibility of attaining the nutrients removal efficiency of 98% for PO_4^{3-} (the most removed pollutant) and 40% for $NO_3^- + NH_4^+$ (the least removed pollutant) in tested Fe^0-supported AD systems for domestic sewage. The effectiveness of the Fe^0-supported AD system to remove PO_4^{3-} is probably mainly contributed by the enhanced precipitation and adsorption of phosphorus by the FeCPs. The relatively low performance of the Fe^0-supported AD system to remove $NO_3^- + NH_4^+$ is conceivably due to the abiotic conversion of some nitrate to ammonium by Fe^0 materials. The research findings suggest that the iron scraps which are normally regarded as wastes can be used in Fe^0-supported AD systems for performance improvement. The dissolution of Fe^0 material depends on the type of Fe^0 materials and the characteristics of the dissolving media.

Therefore case-to-case optimisation studies of materials should be carried out to acquire the desired output. Mixing of the reactants, monitoring of qualities and quantities of biogas and sludge, and depletion of substrates in the reactors were noted as the limitations of this study. Therefore, the limitations are considered as the motive for the continuation of this study.

References

1. Melidis, P.; Vaiopoulou, E.; Athanasoulia, E.; Aivasidis, A. Anaerobic treatment of domestic wastewater using an anaerobic fixed-bed loop reactor. *Desalination* **2009**, *248*, 716–722. [CrossRef]
2. Alexiou, G.; Mara, D. Anaerobic waste stabilization ponds. *Appl. Biochem. Biotechnol.* **2003**, *109*, 241–252. [CrossRef]
3. Moran, S. *An Applied Guide to Water and Effluent Treatment Plant Design*; Butterworth-Heinemann: Oxford, UK, 2018. [CrossRef]
4. Kujawa-Roeleveld, K.; Zeeman, G. Anaerobic Treatment in Decentralised and Source-Separation-Based Sanitation Concepts. *Rev. Environ. Sci. Bio/Technol.* **2006**, *5*, 115–139. [CrossRef]
5. Riffat, R.; Husnain, T. *Fundamentals of Wastewater Treatment and Engineering*; CRC Press: Boca Raton, FL, USA, 2013. [CrossRef]
6. Tchobanoglous, G. *Wastewater Engineering: Treatment and Resource Recovery*; McGraw-Hill: New York, NY, USA, 2014; Volume 2.
7. Diatta, J.; Waraczewska, Z.; Grzebisz, W.; Niewiadomska, A.; Tatuśko-Krygier, N. Eutrophication Induction Via N/P and P/N Ratios Under Controlled Conditions—Effects of Temperature and Water Sources. *Water Air Soil Pollut.* **2020**, *231*, 149. [CrossRef]
8. Hendriks, A.; Zeeman, G. Pretreatments to enhance the digestibility of lignocellulosic biomass. *Bioresour. Technol.* **2009**, *100*, 10–18. [CrossRef]
9. Shah, F.A.; Mahmood, Q.; Rashid, N.; Pervez, A.; Raja, I.A.; Shah, M.M. Co-digestion, pretreatment and digester design for enhanced methanogenesis. *Renew. Sustain. Energy Rev.* **2015**, *42*, 627–642. [CrossRef]
10. Karki, R.; Chuenchart, W.; Surendra, K.; Shrestha, S.; Raskin, L.; Sung, S.; Hashimoto, A.; Khanal, S.K. Anaerobic co-digestion: Current status and perspectives. *Bioresour. Technol.* **2021**, *330*, 125001. [CrossRef]
11. Romero-Güiza, M.; Vila, J.; Mata-Alvarez, J.; Chimenos, J.M.; Astals, S. The role of additives on anaerobic digestion: A review. *Renew. Sustain. Energy Rev.* **2016**, *58*, 1486–1499. [CrossRef]
12. Wu, D.; Zheng, S.; Ding, A.; Sun, G.; Yang, M. Performance of a zero valent iron-based anaerobic system in swine wastewater treatment. *J. Hazard. Mater.* **2015**, *286*, 1–6. [CrossRef]
13. Deng, S.; Peng, S.; Xie, B.; Yang, X.; Sun, S.; Yao, H.; Li, D. Influence characteristics and mechanism of organic carbon on denitrification, N_2O emission and NO_2-Accumulation in the iron [Fe (0)]-oxidizing supported autotrophic denitrification process. *Chem. Eng. J.* **2020**, *393*, 124736.
14. Fu, F.; Dionysiou, D.D.; Liu, H. The use of zero-valent iron for groundwater remediation and wastewater treatment: A review. *J. Hazard. Mater.* **2014**, *267*, 194–205. [CrossRef]
15. Feng, Y.; Zhang, Y.; Quan, X.; Chen, S. Enhanced anaerobic digestion of waste activated sludge digestion by the addition of zero valent iron. *Water Res.* **2014**, *52*, 242–250. [CrossRef]
16. Yuan, T.; Bian, S.; Ko, J.H.; Liu, J.; Shi, X.; Xu, Q. Exploring the roles of zero-valent iron in two-stage food waste anaerobic digestion. *Waste Manag.* **2020**, *107*, 91–100. [CrossRef]
17. Kong, X.; Wei, Y.; Xu, S.; Liu, J.; Li, H.; Liu, Y.; Yu, S. Inhibiting excessive acidification using zero-valent iron in anaerobic digestion of food waste at high organic load rates. *Bioresour. Technol.* **2016**, *211*, 65–71. [CrossRef]
18. Domrongpokkaphan, V.; Phalakornkule, C.; Khemkhao, M. In-situ methane enrichment of biogas from anaerobic digestion of palm oil mill effluent by addition of zero valent iron (ZVI). *Int. J. Hydrogen Energy* **2021**, *46*, 30976–30987. [CrossRef]
19. Meng, X.; Zhang, Y.; Li, Q.; Quan, X. Adding Fe^0 powder to enhance the anaerobic conversion of propionate to acetate. *Biochem. Eng. J.* **2013**, *73*, 80–85. [CrossRef]

20. Zhang, Y.; Jing, Y.; Quan, X.; Liu, Y.; Onu, P. A built-in zero valent iron anaerobic reactor to enhance treatment of azo dye wastewater. *Water Sci. Technol.* **2011**, *63*, 741–746. [CrossRef]
21. Liu, Y.; Zhang, Y.; Quan, X.; Li, Y.; Zhao, Z.; Meng, X.; Chen, S. Optimization of anaerobic acidogenesis by adding Fe^0 powder to enhance anaerobic wastewater treatment. *Chem. Eng. J.* **2012**, *192*, 179–185. [CrossRef]
22. Zang, Y.; Yang, Y.; Hu, Y.; Ngo, H.H.; Wang, X.C.; Li, Y.-Y. Zero-valent iron enhanced anaerobic digestion of pre-concentrated domestic wastewater for bioenergy recovery: Characteristics and mechanisms. *Bioresour. Technol.* **2020**, *310*, 123441. [CrossRef]
23. Till, B.A.; Weathers, L.J.; Alvarez, P.J.J. Fe(0)-Supported Autotrophic Denitrification. *Environ. Sci. Technol.* **1998**, *32*, 634–639. [CrossRef]
24. Kato, S.; Hashimoto, K.; Watanabe, K. Methanogenesis facilitated by electric syntrophy via (semi)conductive iron-oxide minerals. *Environ. Microbiol.* **2012**, *14*, 1646–1654. [CrossRef]
25. Zhou, S.; Xu, J.; Yang, G.; Zhuang, L. Methanogenesis affected by the co-occurrence of iron(III) oxides and humic substances. *FEMS Microbiol. Ecol.* **2014**, *88*, 107–120. [CrossRef]
26. Yamada, C.; Kato, S.; Ueno, Y.; Ishii, M.; Igarashi, Y. Conductive iron oxides accelerate thermophilic methanogenesis from acetate and propionate. *J. Biosci. Bioeng.* **2015**, *119*, 678–682. [CrossRef]
27. Hwang, Y.; Sivagurunathan, P.; Lee, M.-K.; Yun, Y.-M.; Song, Y.-C.; Kim, D.-H. Enhanced hydrogen fermentation by zero valent iron addition. *Int. J. Hydrogen Energy* **2019**, *44*, 3387–3394. [CrossRef]
28. Lufingo, M.; Ndé-Tchoupé, A.I.; Hu, R.; Njau, K.N.; Noubactep, C. A Novel and Facile Method to Characterize the Suitability of Metallic Iron for Water Treatment. *Water* **2019**, *11*, 2465. [CrossRef]
29. Sun, Y.; Li, J.; Huang, T.; Guan, X. The influences of iron characteristics, operating conditions and solution chemistry on contaminants removal by zero-valent iron: A review. *Water Res.* **2016**, *100*, 277–295. [CrossRef]
30. Xu, Y.; Wang, C.; Hou, J.; Wang, P.; You, G.; Miao, L.; Lv, B.; Yang, Y.; Zhang, F. Application of zero valent iron coupling with biological process for wastewater treatment: A review. *Rev. Environ. Sci. Bio/Technol.* **2017**, *16*, 667–693. [CrossRef]
31. Xiao, M.; Hu, R.; Ndé-Tchoupé, A.I.; Gwenzi, W.; Noubactep, C. Metallic Iron for Water Remediation: Plenty of Room for Collaboration and Convergence to Advance the Science. *Water* **2022**, *14*, 1492. [CrossRef]
32. Konadu-Amoah, B.; Hu, R.; Ndé-Tchoupé, A.I.; Gwenzi, W.; Noubactep, C. Metallic iron (Fe^0)-based materials for aqueous phosphate removal: A critical review. *J. Environ. Manag.* **2022**, *315*, 115157.
33. Yu, X.; Amrhein, C.; Deshusses, M.A.; Matsumoto, M. Perchlorate Reduction by Autotrophic Bacteria in the Presence of Zero-Valent Iron. *Environ. Sci. Technol.* **2006**, *40*, 1328–1334. [CrossRef]
34. Yu, X.; Amrhein, C.; Deshusses, M.A.; Matsumoto, M.R. Perchlorate Reduction by Autotrophic Bacteria Attached to Zerovalent Iron in a Flow-Through Reactor. *Environ. Sci. Technol.* **2007**, *41*, 990–997. [CrossRef] [PubMed]
35. Deng, S.; Li, D.; Yang, X.; Xing, W.; Li, J.; Zhang, Q. Biological denitrification process based on the Fe(0)–carbon micro-electrolysis for simultaneous ammonia and nitrate removal from low organic carbon water under a microaerobic condition. *Bioresour. Technol.* **2016**, *219*, 677–686. [CrossRef] [PubMed]
36. Bai, H.; Kang, Y.; Quan, H.; Han, Y.; Sun, J.; Feng, Y. Bioremediation of copper-containing wastewater by sulfate reducing bacteria coupled with iron. *J. Environ. Manag.* **2013**, *129*, 350–356. [CrossRef] [PubMed]
37. Boontian, N. Effect of Zero Valent Iron (ZVI) in Wastewater Treatment: A Review. *Appl. Mech. Mater.* **2015**, *775*, 180–184. [CrossRef]
38. Noubactep, C.; Meinrath, G.; Dietrich, P.; Sauter, M.; Merkel, B.J. Testing the Suitability of Zerovalent Iron Materials for Reactive Walls. *Environ. Chem.* **2005**, *2*, 71–76. [CrossRef]
39. Hu, R.; Cui, X.; Xiao, M.; Qiu, P.; Lufingo, M.; Gwenzi, W.; Noubactep, C. Characterizing the Suitability of Granular Fe^0 for the Water Treatment Industry. *Processes* **2019**, *7*, 652. [CrossRef]
40. Chen, Y.-M.; Li, C.-W.; Chen, S.-S. Fluidized zero valent iron bed reactor for nitrate removal. *Chemosphere* **2005**, *59*, 753–759. [CrossRef]
41. Antwi, P.; Li, J.; Boadi, P.O.; Meng, J.; Shi, E.; Chi, X.; Deng, K.; Ayivi, F. Dosing effect of zero valent iron (ZVI) on biomethanation and microbial community distribution as revealed by 16S rRNA high-throughput sequencing. *Int. Biodeterior. Biodegrad.* **2017**, *123*, 191–199. [CrossRef]
42. Zhao, L.; Ji, Y.; Kong, D.; Lu, J.; Zhou, Q.; Yin, X. Simultaneous removal of bisphenol A and phosphate in zero-valent iron activated persulfate oxidation process. *Chem. Eng. J.* **2016**, *303*, 458–466. [CrossRef]
43. Charalambous, P.; Vyrides, I. In situ biogas upgrading and enhancement of anaerobic digestion of cheese whey by addition of scrap or powder zero-valent iron (ZVI). *J. Environ. Manag.* **2021**, *280*, 111651. [CrossRef]
44. Hu, R.; Ndé-Tchoupé, A.I.; Lufingo, M.; Xiao, M.; Nassi, A.; Noubactep, C.; Njau, K.N. The impact of selected pretreatment procedures on iron dissolution from metallic iron specimens used in water treatment. *Sustainability* **2019**, *11*, 671. [CrossRef]
45. Günther, S.; Koch, C.; Hübschmann, T.; Röske, I.; Müller, R.A.; Bley, T.; Harms, H.; Müller, S. Correlation of Community Dynamics and Process Parameters As a Tool for the Prediction of the Stability of Wastewater Treatment. *Environ. Sci. Technol.* **2012**, *46*, 84–92. [CrossRef]
46. Aly, M.; Hashmi, M.S.J.; Olabi, A.G.; Benyounis, K.Y.; Messeiry, M.; Hussain, A.; Abadir, E.F. Optimization of Alkaline Treatment Conditions of Flax Fiber Using Box–Behnken Method. *J. Nat. Fibers* **2012**, *9*, 256–276. [CrossRef]
47. Akteke-Ozturk, B.; Koksal, G.; Weber, G.-W. Nonconvex optimization of desirability functions. *Qual. Eng.* **2018**, *30*, 293–310. [CrossRef]

48.　Summer, D.; Schöftner, P.; Watzinger, A.; Reichenauer, T.G. Inhibition and stimulation of two perchloroethene degrading bacterial cultures by nano- and micro-scaled zero-valent iron particles. *Sci. Total Environ.* **2020**, *722*, 137802. [CrossRef]

49.　Li, J.; Dou, X.; Qin, H.; Sun, Y.; Yin, D.; Guan, X. Characterization methods of zerovalent iron for water treatment and remediation. *Water Res.* **2019**, *148*, 70–85. [CrossRef]

50.　Li, S.; Ding, Y.; Wang, W.; Lei, H. A facile method for determining the Fe(0) content and reactivity of zero valent iron. *Anal. Methods* **2016**, *8*, 1239–1248. [CrossRef]

51.　Mudhoo, A.; Kumar, S. Effects of heavy metals as stress factors on anaerobic digestion processes and biogas production from biomass. *Int. J. Environ. Sci. Technol.* **2013**, *10*, 1383–1398. [CrossRef]

52.　Abdel-Shafy, H.I.; Mansour, M.S. Biogas production as affected by heavy metals in the anaerobic digestion of sludge. *Egypt. J. Pet.* **2014**, *23*, 409–417. [CrossRef]

53.　Alrawashdeh, K.A.B.; Gul, E.; Yang, Q.; Yang, H.; Bartocci, P.; Fantozzi, F. Effect of Heavy Metals in the Performance of Anaerobic Digestion of Olive Mill Waste. *Processes* **2020**, *8*, 1146. [CrossRef]

54.　Chen, S.Y.; Chen, W.-H.; Shih, C.J. Heavy metal removal from wastewater using zero-valent iron nanoparticles. *Water Sci. Technol.* **2008**, *58*, 1947–1954. [CrossRef]

55.　Fu, F.; Han, W.; Tang, B.; Hu, M.; Cheng, Z. Insights into environmental remediation of heavy metal and organic pollutants: Simultaneous removal of hexavalent chromium and dye from wastewater by zero-valent iron with ligand-enhanced reactivity. *Chem. Eng. J.* **2013**, *232*, 534–540. [CrossRef]

56.　Konadu-Amoah, B.; Ndé-Tchoupé, A.I.; Hu, R.; Gwenzi, W.; Noubactep, C. Investigating the Fe^0/H_2O systems using the methylene blue method: Validity, applications, and future directions. *Chemosphere* **2022**, *291*, 132913.

57.　Noubactep, C. On the mechanism of microbe inactivation by metallic iron. *J. Hazard. Mater.* **2011**, *198*, 383–386. [CrossRef]

58.　You, Y.; Han, J.; Chiu, P.C.; Jin, Y. Removal and Inactivation of Waterborne Viruses Using Zerovalent Iron. *Environ. Sci. Technol.* **2005**, *39*, 9263–9269. [CrossRef]

59.　Latif, M.A.; Mehta, C.; Batstone, D.J. Low pH anaerobic digestion of waste activated sludge for enhanced phosphorous release. *Water Res.* **2015**, *81*, 288–293. [CrossRef]

60.　Mehta, C.M.; Batstone, D. Nutrient solubilization and its availability following anaerobic digestion. *Water Sci. Technol.* **2013**, *67*, 756–763. [CrossRef]

61.　Martí, N.; Bouzas, A.; Seco, A.; Ferrer, J. Struvite precipitation assessment in anaerobic digestion processes. *Chem. Eng. J.* **2008**, *141*, 67–74. [CrossRef]

62.　Lin, H.; Gan, J.; Rajendran, A.; Reis, C.E.R.; Hu, B. Phosphorus Removal and Recovery from Digestate after Biogas Production. In *Biofuels-Status and Perspective*; IntechOpen: London, UK, 2015. [CrossRef]

63.　Schievano, A.; D'Imporzano, G.; Salati, S.; Adani, F. On-field study of anaerobic digestion full-scale plants (Part I): An on-field methodology to determine mass, carbon and nutrients balance. *Bioresour. Technol.* **2011**, *102*, 7737–7744. [CrossRef]

64.　Akunna, J.C. *Anaerobic Waste-Wastewater Treatment and Biogas Plants: A Practical Handbook*; CRC Press: Boca Raton, FL, USA, 2018.

65.　Schädler, S.; Burkhardt, C.; Hegler, F.; Straub, K.L.; Miot, J.; Benzerara, K.; Kappler, A. Formation of Cell-Iron-Mineral Aggregates by Phototrophic and Nitrate-Reducing Anaerobic Fe(II)-Oxidizing Bacteria. *Geomicrobiol. J.* **2009**, *26*, 93–103. [CrossRef]

66.　Yin, W.; Wu, J.; Li, P.; Wang, X.; Zhu, N.; Wu, P.; Yang, B. Experimental study of zero-valent iron induced nitrobenzene reduction in groundwater: The effects of pH, iron dosage, oxygen and common dissolved anions. *Chem. Eng. J.* **2012**, *184*, 198–204. [CrossRef]

67.　Sleiman, N.; Deluchat, V.; Wazne, M.; Mallet, M.; Courtin-Nomade, A.; Kazpard, V.; Baudu, M. Phosphate removal from aqueous solutions using zero valent iron (ZVI): Influence of solution composition and ZVI aging. *Colloids Surfaces A Physicochem. Eng. Asp.* **2017**, *514*, 1–10. [CrossRef]

68.　Wang, Q.; Liao, Z.; Yao, D.; Yang, Z.; Wu, Y.; Tang, C. Phosphorus immobilization in water and sediment using iron-based materials: A review. *Sci. Total Environ.* **2021**, *767*, 144246. [CrossRef] [PubMed]

69.　Xiao, X.; Sheng, G.-P.; Mu, Y.; Yu, H.-Q. A modeling approach to describe ZVI-based anaerobic system. *Water Res.* **2013**, *47*, 6007–6013. [CrossRef]

70.　Kassab, G.; Khater, D.; Odeh, F.; Shatanawi, K.; Halalsheh, M.; Arafah, M.; Van Lier, J.B. Impact of Nanoscale Magnetite and Zero Valent Iron on the Batch-Wise Anaerobic Co-Digestion of Food Waste and Waste-Activated Sludge. *Water* **2020**, *12*, 1283. [CrossRef]

71.　Kong, X.; Niu, J.; Zhang, W.; Liu, J.; Yuan, J.; Li, H.; Yue, X. Mini art review for zero valent iron application in anaerobic digestion and technical bottlenecks. *Sci. Total Environ.* **2021**, *791*, 148415. [CrossRef] [PubMed]

72.　Ye, W.; Lu, J.; Ye, J.; Zhou, Y. The effects and mechanisms of zero-valent iron on anaerobic digestion of solid waste: A mini-review. *J. Clean. Prod.* **2021**, *278*, 123567. [CrossRef]

73.　Pyae, H.A.; Dararatana, S. Optimizing bio-methanation by differential zero valent iron (ZVI) particle size in cassava pulp feed CSTRs. *Acad. J. Biotechnol.* **2019**, *6*. [CrossRef]

74.　Huang, Y.-X.; Guo, J.; Zhang, C.; Hu, Z. Hydrogen production from the dissolution of nano zero valent iron and its effect on anaerobic digestion. *Water Res.* **2016**, *88*, 475–480. [CrossRef]

75.　Suanon, F.; Sun, Q.; Li, M.; Cai, X.; Zhang, Y.; Yan, Y.; Yu, C.-P. Application of nanoscale zero valent iron and iron powder during sludge anaerobic digestion: Impact on methane yield and pharmaceutical and personal care products degradation. *J. Hazard. Mater.* **2017**, *321*, 47–53. [CrossRef]

76. Zhou, H.; Cao, Z.; Ying, Z.; Liu, J.; Hu, T.; Zhang, M.; Zhang, J. Effects of zero-valent iron and enzymes on the anaerobic co-digestion of sewage sludge and corn silage. *Environ. Prot. Eng.* **2020**, *46*, 41–56. [CrossRef]

77. Hu, R.; Ndé-Tchoupé, A.I.; Cao, V.; Gwenzi, W.; Noubactep, C. Metallic iron for environmental remediation: The fallacy of the electron efficiency concept. *Front. Environ. Chem.* **2021**, *2*, 677813.

78. Bradley, I.; Straub, A.; Maraccini, P.; Markazi, S.; Nguyen, T.H. Iron oxide amended biosand filters for virus removal. *Water Res.* **2011**, *45*, 4501–4510. [CrossRef]

79. Tepong-Tsindé, R.; Ndé-Tchoupé, A.I.; Noubactep, C.; Nassi, A.; Ruppert, H. Characterizing a newly designed steel-wool-based household filter for safe drinking water provision: Hydraulic conductivity and efficiency for pathogen removal. *Processes* **2019**, *7*, 966. [CrossRef]

80. Tsinde, R.T. Designing and Piloting a Household Filter for the Peri-Urban Population of Douala (Cameroon). *Freib. Online Geosci.* **2021**, *61*, 1–90. [CrossRef]

81. Matheson, L.J.; Tratnyek, P.G. Reductive Dehalogenation of Chlorinated Methanes by Iron Metal. *Environ. Sci. Technol.* **1994**, *28*, 2045–2053. [CrossRef]

82. Sarr, D. Zero-Valent-Iron Permeable Reactive Barriers—How Long Will They Last? *Remediation* **2001**, *11*, 1–18.

83. Obiri-Nyarko, F.; Grajales-Mesa, S.J.; Malina, G. An overview of permeable reactive barriers for in situ sustainable groundwater remediation. *Chemosphere* **2014**, *111*, 243–259. [CrossRef]

84. Gheju, M.; Balcu, I. Sustaining the efficiency of the Fe (0)/H_2O system for Cr (VI) removal by MnO_2 amendment. *Chemosphere* **2019**, *214*, 389–398.

85. Antia, D. Water treatment and desalination using the eco-materials n-Fe^0 (ZVI), n-Fe_3O_4, n-$Fe_xO_yH_z$ [mH_2O], and n-Fe^x [Cation] nO_yH_z [Anion] m [rH_2O]. In *Handbook of Nanomaterials and Nanocomposites for Energy and Environmental Applications*; Springer: Berlin/Heidelberg, Germany, 2020; pp. 66–71.

86. Kumar, A.; Ahammed, M.M.; Shaikh, I.N. Zero-valent iron-modified sand filters for greywater treatment. *Int. J. Environ. Sci. Technol.* **2022**, *19*, 1–14. [CrossRef]

87. Tao, R.; Yang, H.; Cui, X.; Xiao, M.; Gatcha-Bandjun, N.; Kenmogne-Tchidjo, J.F.; Lufingo, M.; Konadu Amoah, B.; Tepong-Tsindé, R.; Ndé-Tchoupé, A.I.; et al. The Suitability of Hybrid Fe^0/Aggregate Filtration Systems for Water Treatment. *Water* **2022**, *14*, 260. [CrossRef]

88. Yang, H.; Hu, R.; Ruppert, H.; Noubactep, C. Modeling porosity loss in Fe^0-based permeable reactive barriers with Faraday's law. *Sci. Rep.* **2021**, *11*, 16998. [CrossRef]

89. Schreier, C.G.; Reinhard, M. Transformation of chlorinated organic compounds by iron and manganese powders in buffered water and in landfill leachate. *Chemosphere* **1994**, *29*, 1743–1753. [CrossRef]

90. McGeough, K.L.; Kalin, R.M.; Myles, P. Carbon Disulfide Removal by Zero Valent Iron. *Environ. Sci. Technol.* **2007**, *41*, 4607–4612. [CrossRef]

91. Augustos de Lemos Chernicharo, C.; Von Sperling, M. *Biological Wastewater Treatment in Warm Climate Regions*; IWA Publishing: London, UK, 2005.